

TAS Code Results for the Third High Lift Prediction Workshop

Yasushi Ito, Mitsuhiro Murayama & Kazuomi Yamamoto
Japan Aerospace Exploration Agency (JAXA)

&

Kentaro Tanaka & Tohru Hirai
Ryoyu Systems Co., Ltd.

PID: 011

3rd High Lift Prediction Workshop
Denver, CO June 3-4, 2017



Summary of cases completed: TAS code

Turbulence model:
SA-noft2-R ($C_{rot} = 1$)

Case	Alpha=8, Fully turb, grid study	Alpha=16, Fully turb, grid study	Other
1a (full gap)	YES	YES	
1b (full gap w adaption)	NO	NO	
1c (partial seal)	NO	NO	
1d (partial seal w adaption)	NO	NO	

Case	Polar, Fully turb	Polar, specified transition	Polar, w transition prediction	Other
2a (no nacelle)	YES	NO	NO	
2b (no nacelle w adaption)	NO	NO	NO	
2c (with nacelle)	YES	NO	NO	
2d (with nacelle w adaption)	NO	NO	NO	

Case	2D Verification study	Other
3	YES	

Summary of cases completed: TAS code

Turbulence model:
SA-noft2-R-QCR2000 ($C_{rot} = 1$)

Case	Alpha=8, Fully turb, grid study	Alpha=16, Fully turb, grid study	Other
1a (full gap)	YES	YES	
1b (full gap w adaption)	NO	NO	
1c (partial seal)	NO	NO	
1d (partial seal w adaption)	NO	NO	

Case	Polar, Fully turb	Polar, specified transition	Polar, w transition prediction	Other
2a (no nacelle)	YES	NO	NO	
2b (no nacelle w adaption)	NO	NO	NO	
2c (with nacelle)	YES	NO	NO	
2d (with nacelle w adaption)	NO	NO	NO	

Case	2D Verification study	Other
3	NO	

Summary of code and numerics used



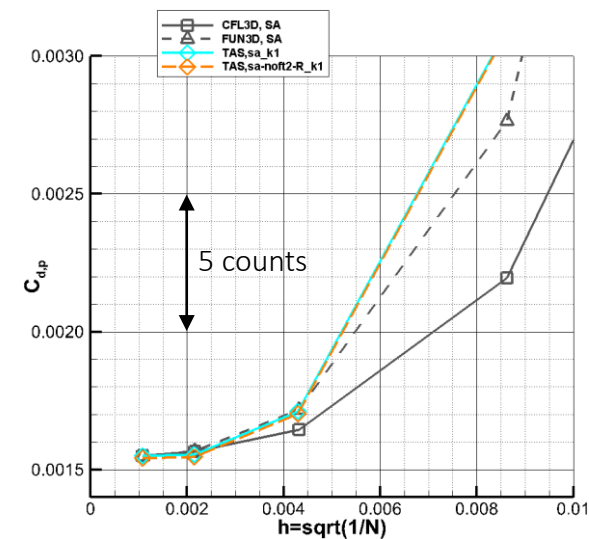
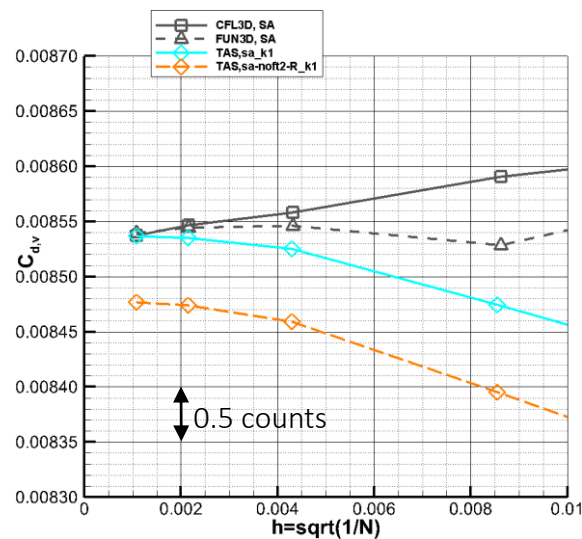
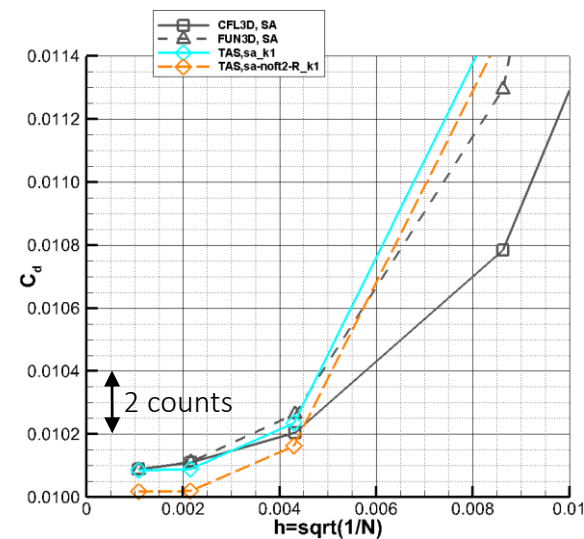
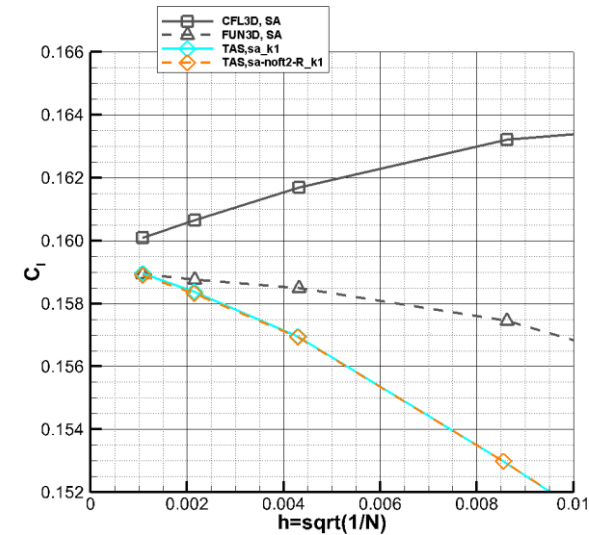
- TAS (Tohoku Univ. Aerodynamic Simulation) code
 - Unstructured hybrid RANS solver
 - Originally developed by Nakahashi *et al.*
- Quadratic Constitutive Relation (QCR) by Spalart
 - Well predicting side-of-body separation in transonic flows based on our previous experience (*e.g.*, Yamamoto *et al.*, AIAA Paper 2010-4222).
 - Evaluated for high-lift cases in this study (also evaluated in HiLiftPW-2).

	TAS code
Grid type	Unstructured hybrid grids
Discretization	Cell-vertex finite volume
Convection flux	HLLEW 2 nd -order with Venkatakrishnan's limiter
Time integration	LU-Symmetric Gauss-Seidel
Turbulence model	SA-noft2-R ($C_{rot} = 1$) (QCR off) or SA-noft2-R-QCR2000 ($C_{rot} = 1$) (QCR on)

Case 3 Verification study results

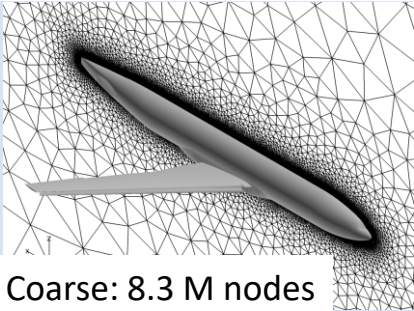
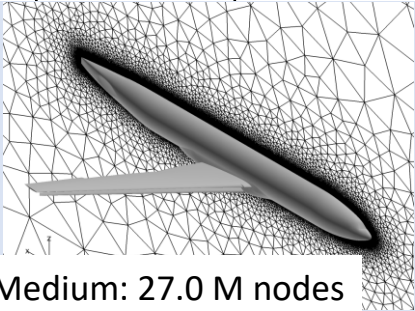
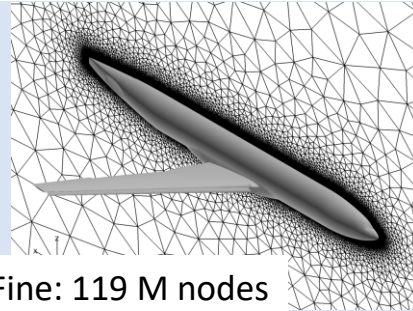
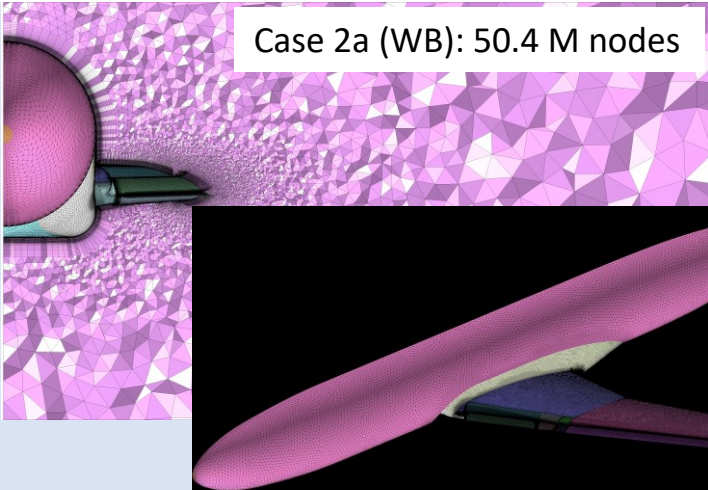
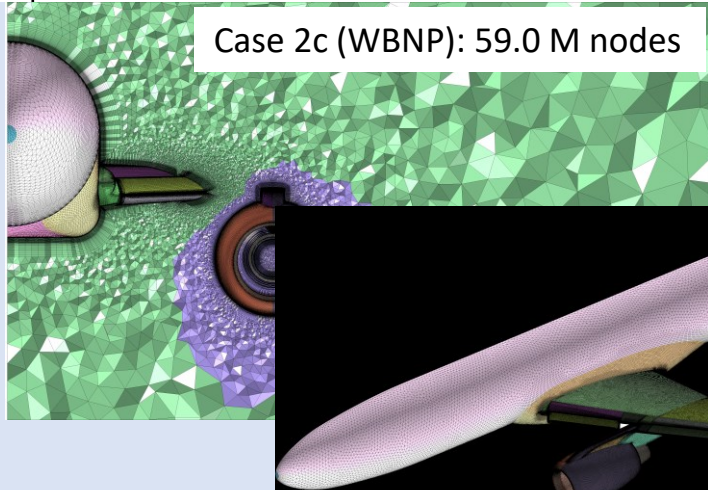


- Based on the finest mesh,
 - Compared w/ FUN3D + SA, TAS code + SA predicts similar C_l & C_d .
 - TAS code + SA-noft2-R ($C_{rot} = 1$) predicts smaller C_d than TAS code + SA by 0.6 drag counts mostly because of the difference in $C_{d,v}$.



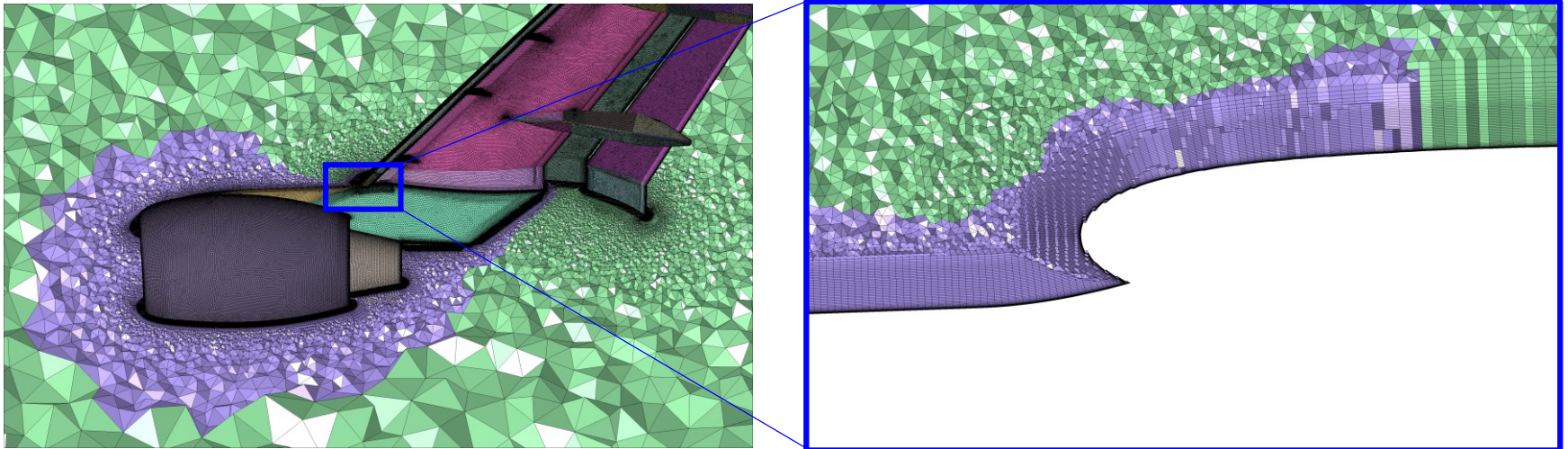
Brief overview of grid systems



Grid System	Case(s)	Problems/Issues
Committee (B3-HLCRM_UnstrHexPrismPyrTet_PW)	1a	Grid quality OK Submitted feedback
 Coarse: 8.3 M nodes	 Medium: 27.0 M nodes	 Fine: 119 M nodes
Committee (D-JSM_UnstrMixed_JAXA)	2a 2c	Wing deformation effect? Mesh resolution enough to predict C_{Lmax} ?
 Case 2a (WB): 50.4 M nodes	 Case 2c (WBNP): 59.0 M nodes	

MEGG3D – Mixed Element Grid Generator in 3D

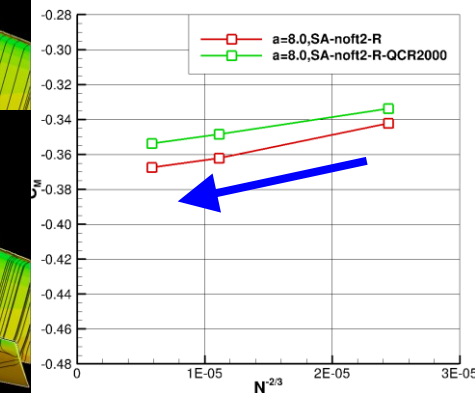
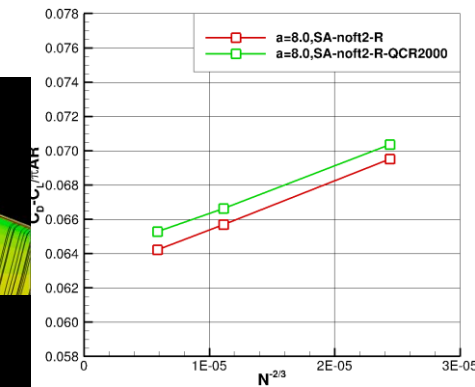
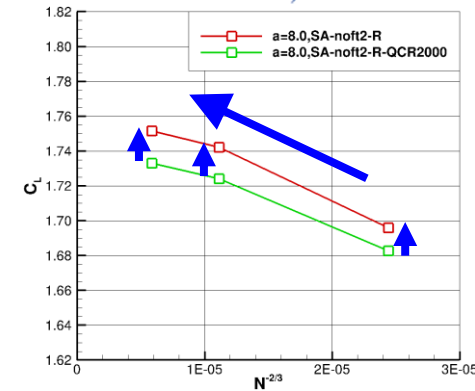
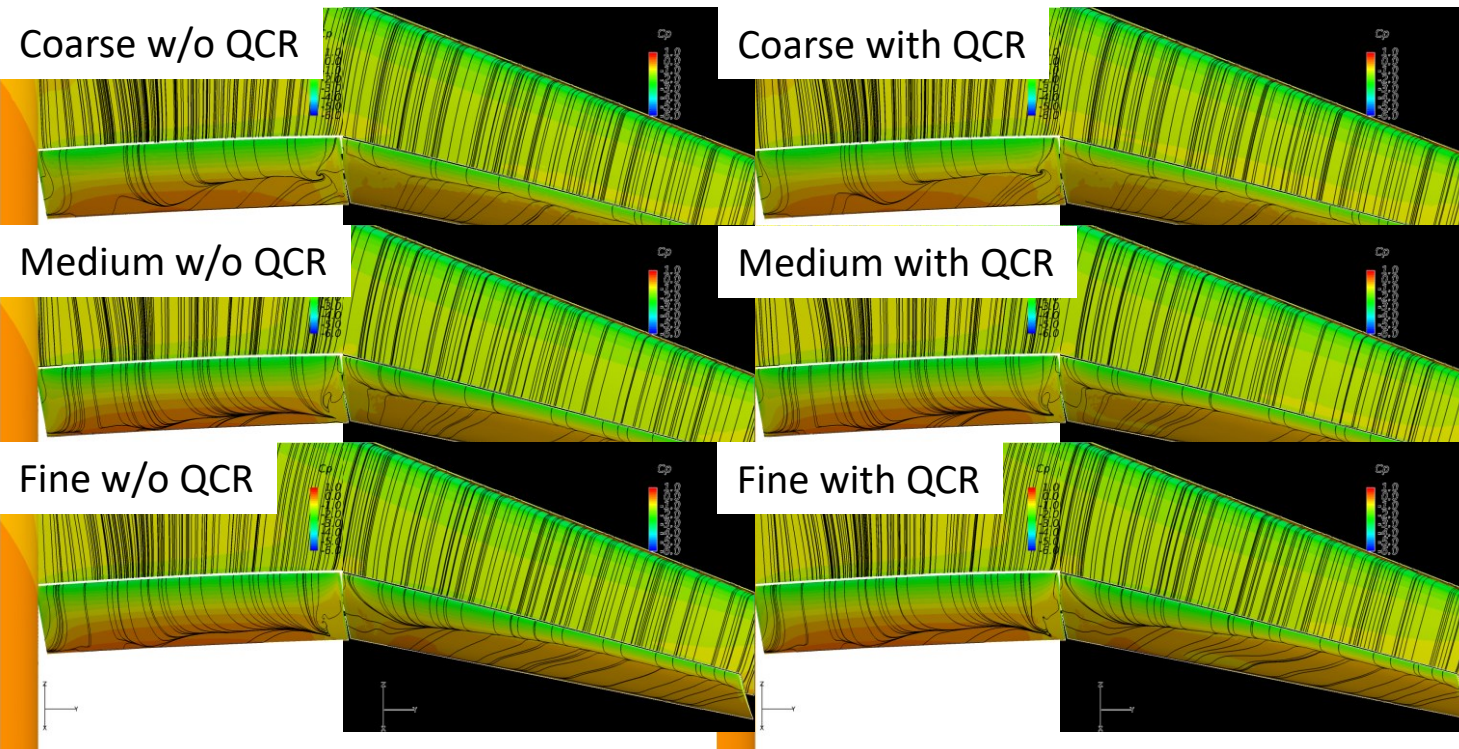
- Unstructured hybrid surface/volume grid generator (prisms, hexes, tets & pyramids)
- The **Automatic Local Remeshing** enabled to reuse a volume grid generated around a baseline geometry (in this case, WB) when an additional geometry (NP) was inserted.
 - New grids were generated automatically.
 - The same elements were used except those around the additional geometry, so that its effect can be evaluated more precisely.



Case 1a HL-CRM $\alpha = 8^\circ$



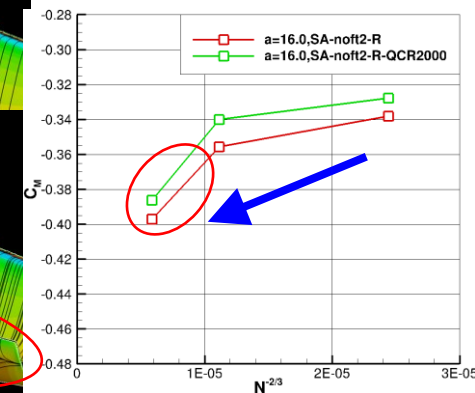
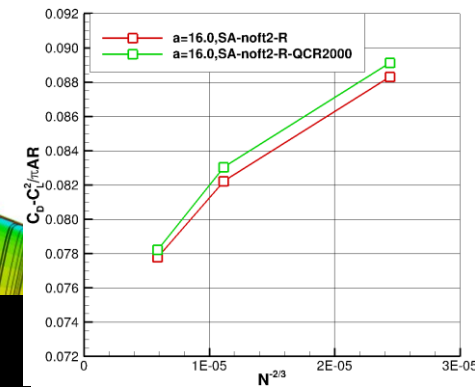
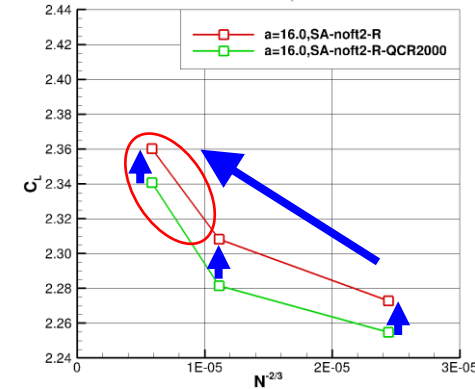
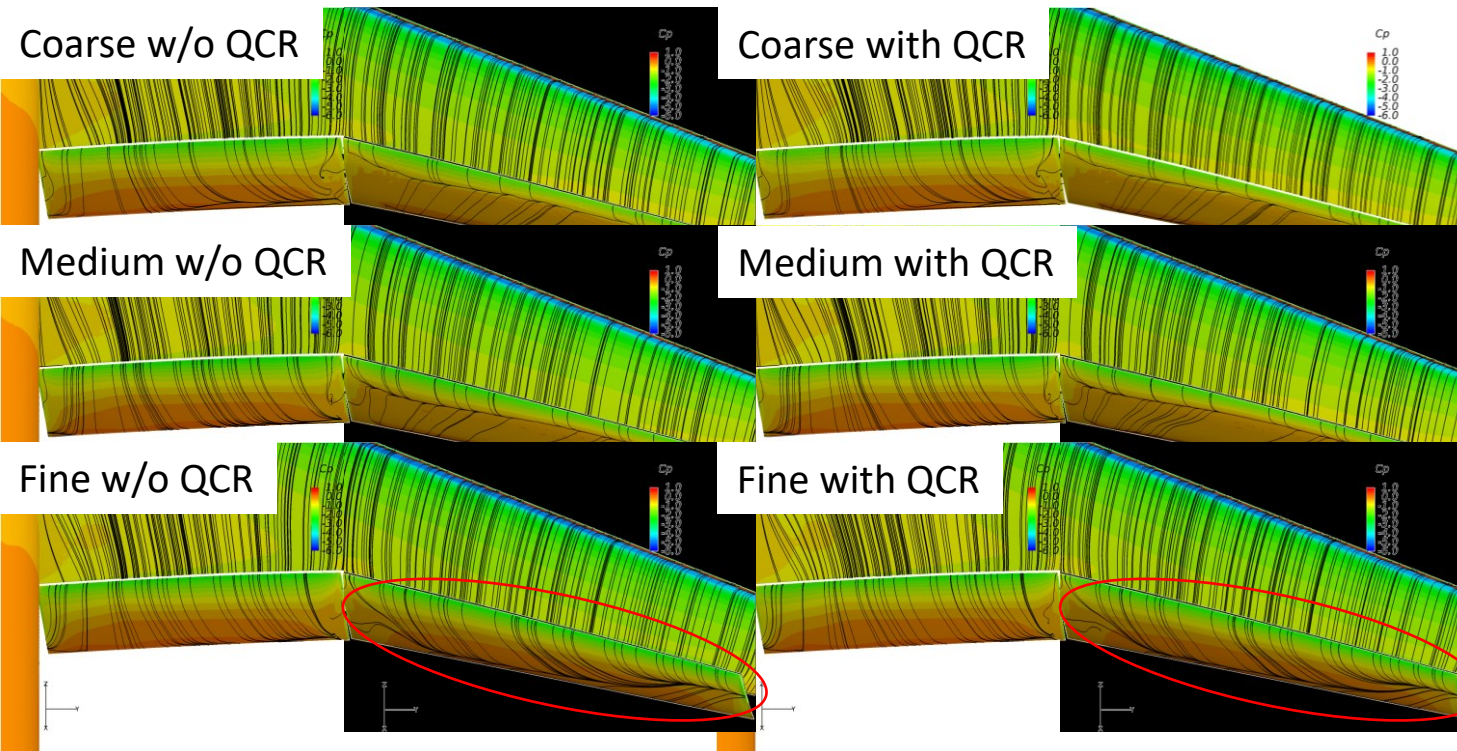
- Large flow separation predicted on the flaps.
- Smaller flow separation on the flaps with a finer mesh. \rightarrow Larger C_L & smaller C_M
- Slightly smaller flow separation predicted by the cases w/o QCR.



Case 1a HL-CRM $\alpha = 16^\circ$

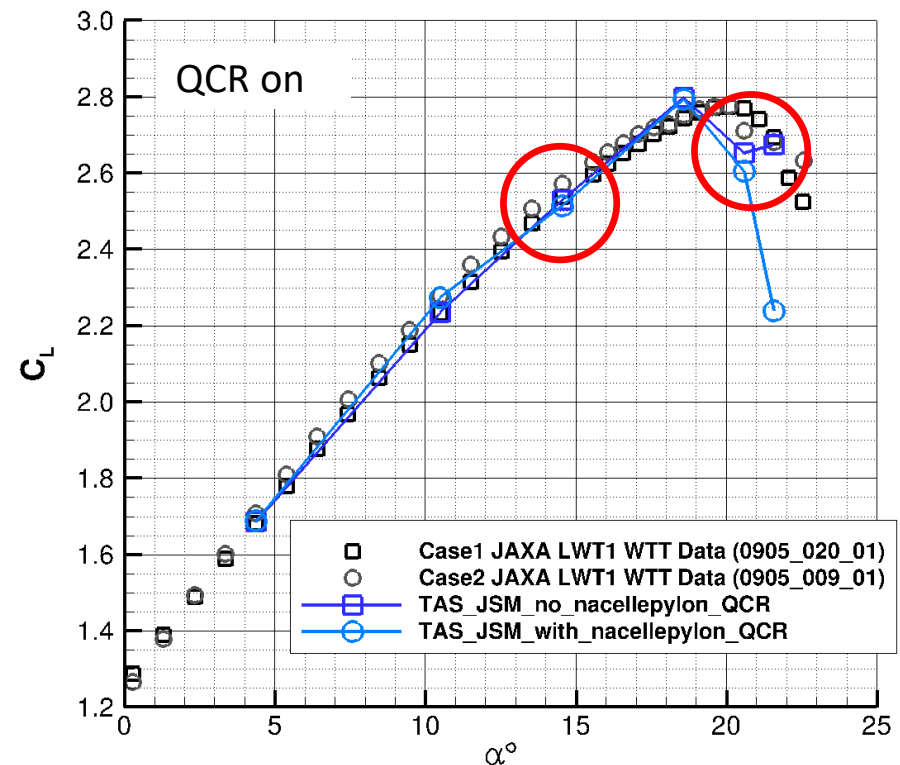
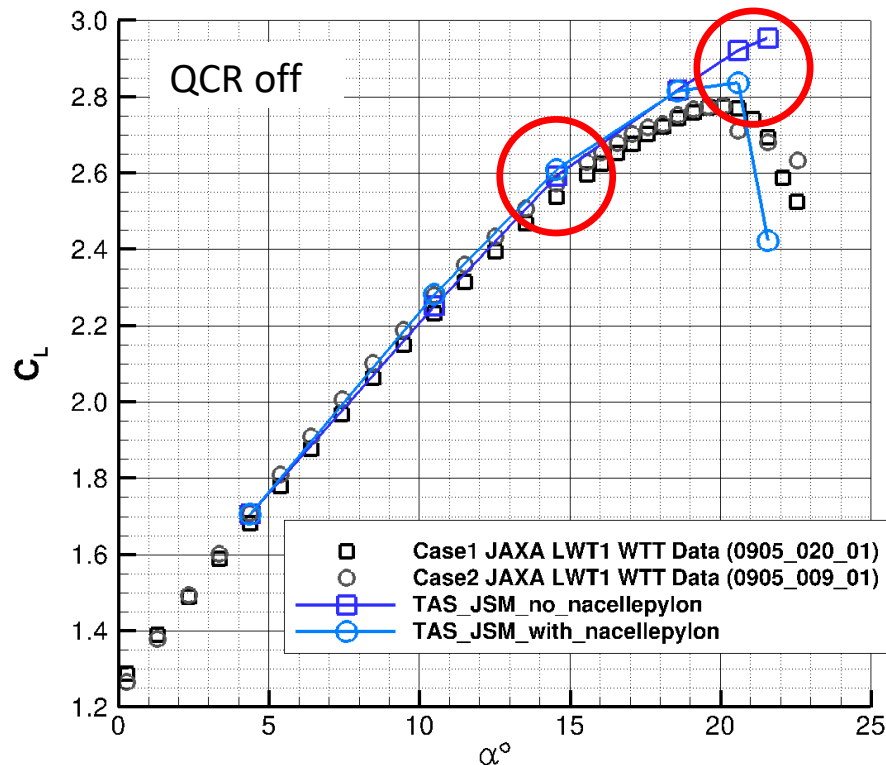


- Smaller flow separation predicted by a finer mesh and by SA w/o QCR.
- With the fine mesh, flow separation almost disappears on the inboard flap & small flow separation on the outboard flap.

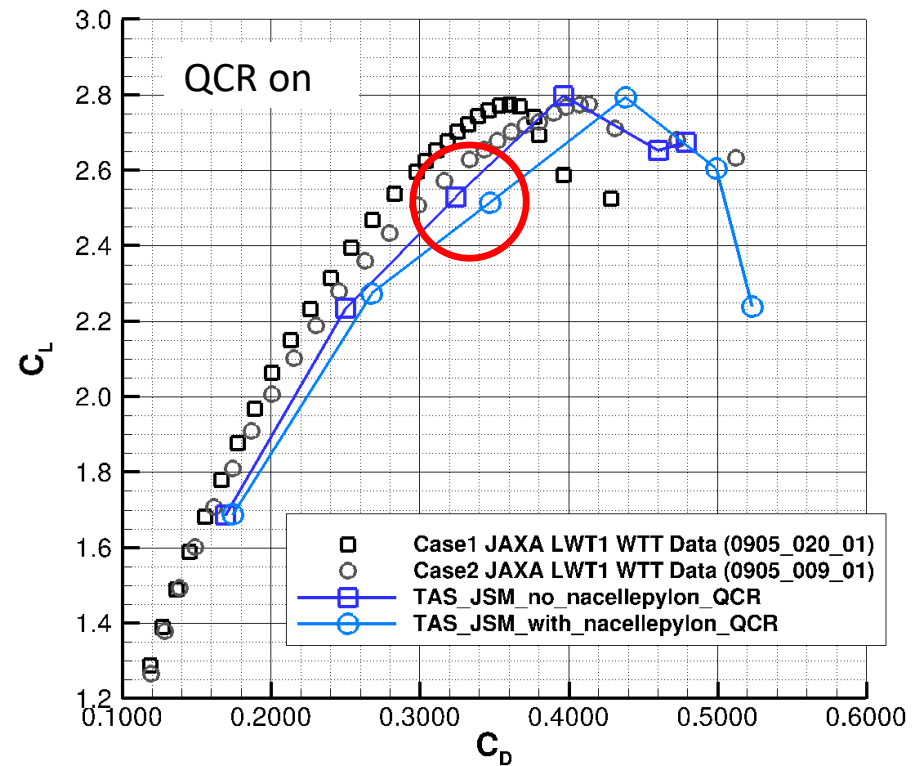
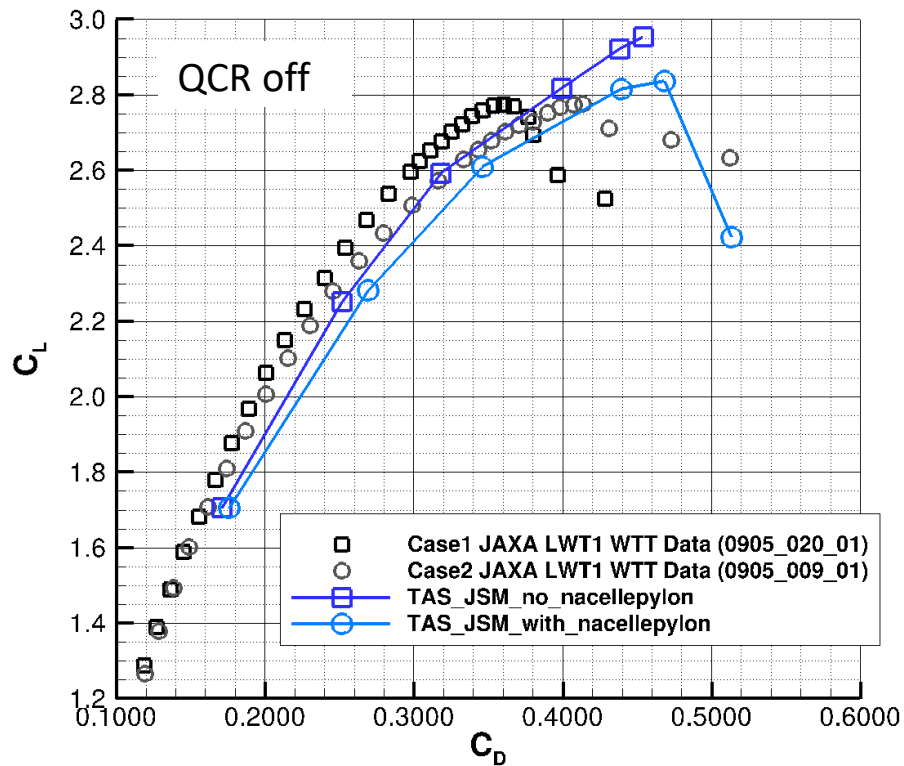


Cases 2a & 2c JSM C_L - α

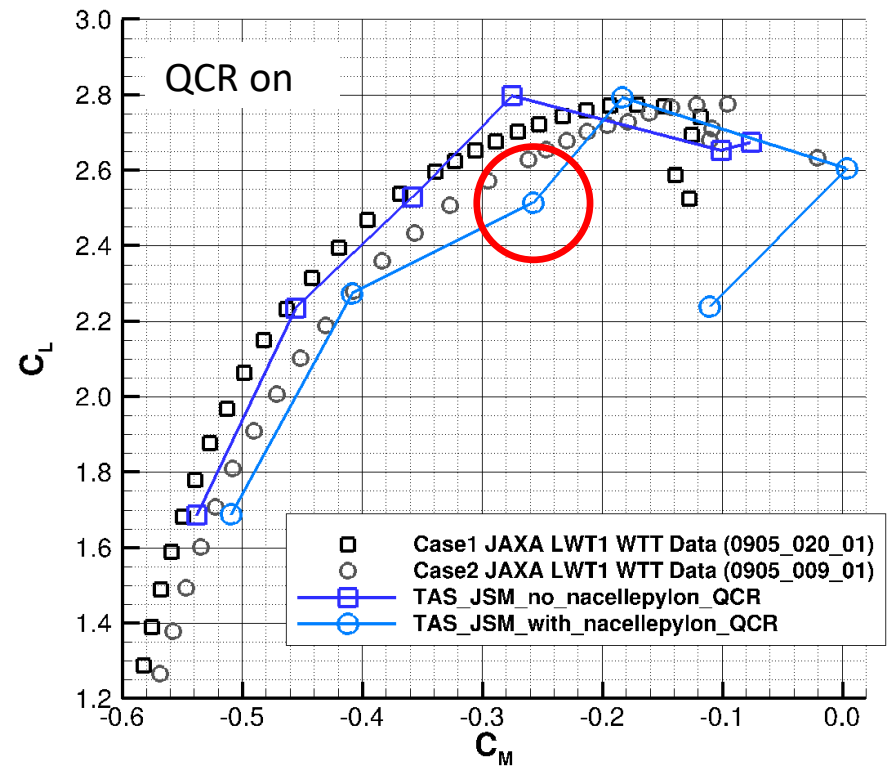
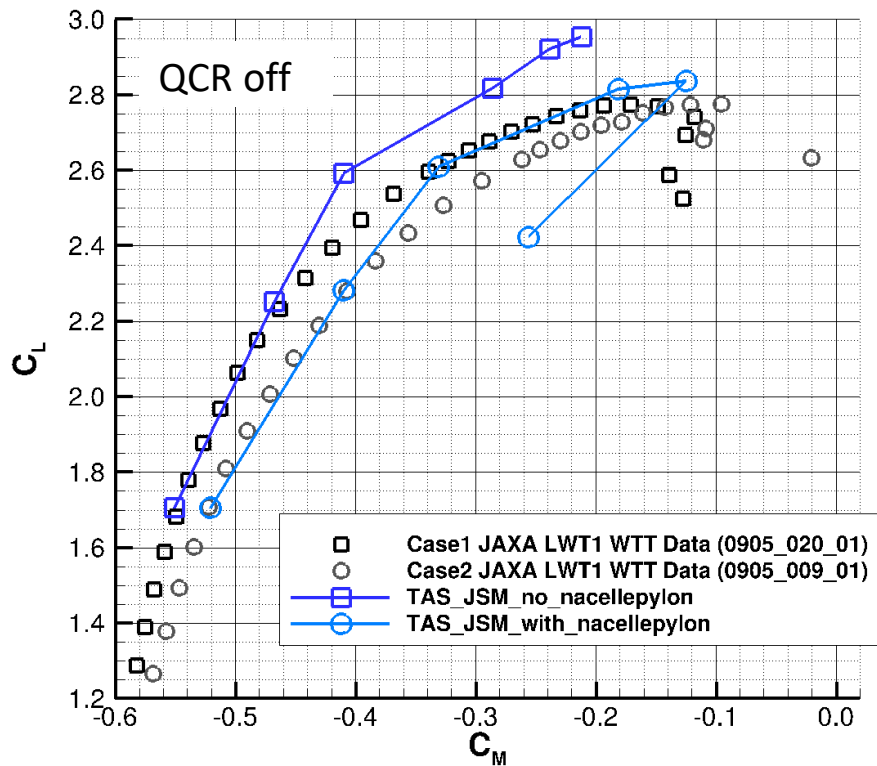
- Difference in C_L at high α due to larger flow separation on the outboard wing when QCR is turned on.



Cases 2a & 2c – JSM C_L - C_D



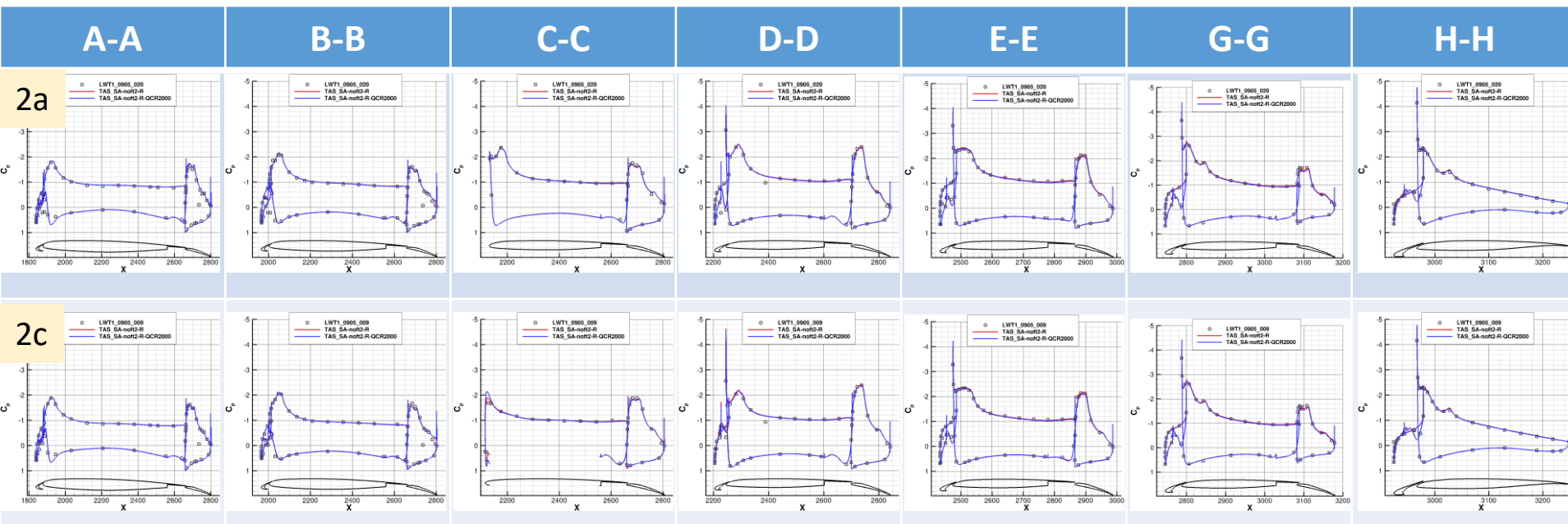
Cases 2a & 2c – JSM C_L - C_M



Cases 2a & 2c – JSM C_p $\alpha = 4.36^\circ$

- Both QCR on/off mostly agree well with experiment.
- QCR on predicts flow separations slightly larger (not visible in the C_p graphs).
- Compared with experiment, a similar tendency was observed at $\alpha = 10.47^\circ$.

— QCR off
— QCR on



Cases 2a & 2c – JSM $\alpha = 4.36^\circ$

- Similar oil flow images

Exp

QCR off

QCR on

Case 2a

C_f
0.025
0.020
0.015
0.010
0.005
0.000

C_f
0.025
0.020
0.015
0.010
0.005
0.000

Case 2c

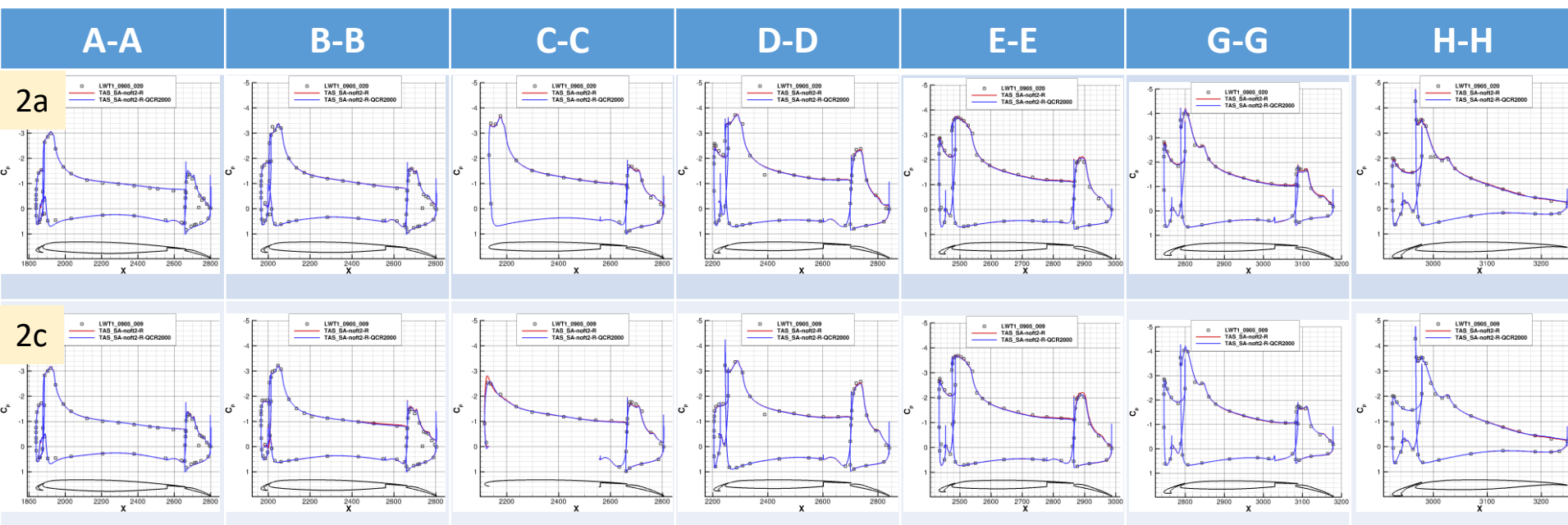
C_f
0.025
0.020
0.015
0.010
0.005
0.000

C_f
0.025
0.020
0.015
0.010
0.005
0.000

Cases 2a & 2c – JSM $C_p \alpha = 10.47^\circ$

- Both QCR on/off mostly agree well with experiment.

— QCR off
— QCR on



Cases 2a & 2c – JSM $\alpha = 10.47^\circ$

- Similar oil flow images

Exp

QCR off

QCR on

Case 2a

C_f
0.025
0.020
0.015
0.010
0.005
0.000

C_f
0.025
0.020
0.015
0.010
0.005
0.000

Case 2c

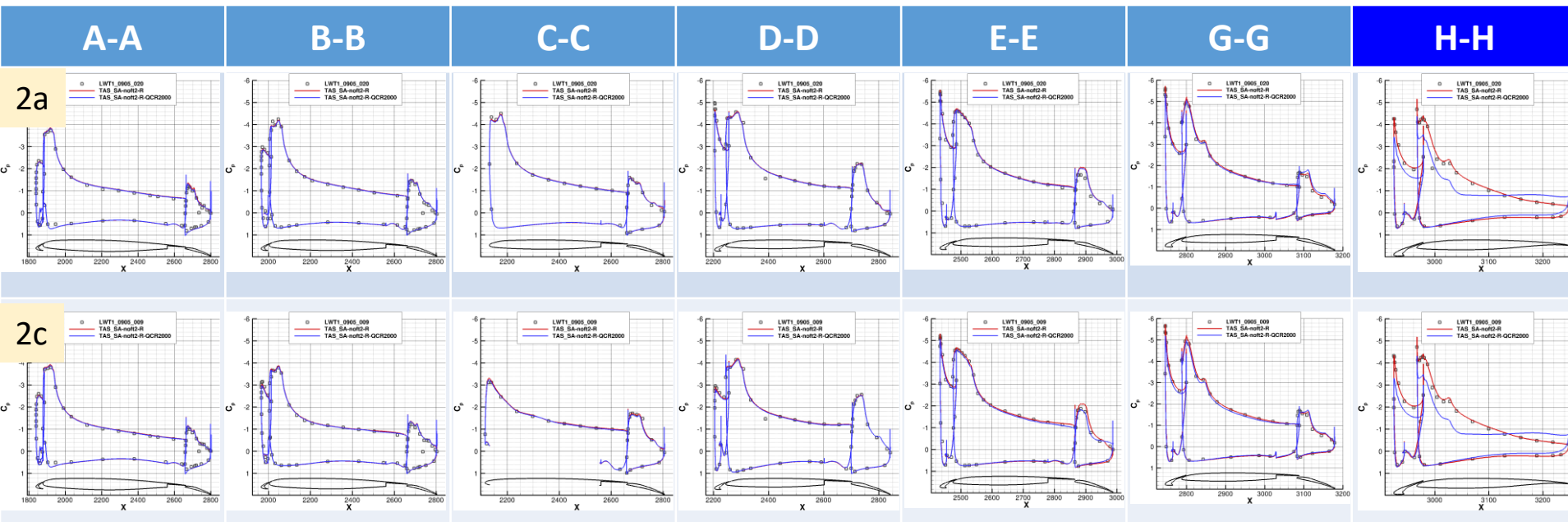
C_f
0.025
0.020
0.015
0.010
0.005
0.000

C_f
0.025
0.020
0.015
0.010
0.005
0.000

Cases 2a & 2c – JSM $C_p \alpha = 14.54^\circ$

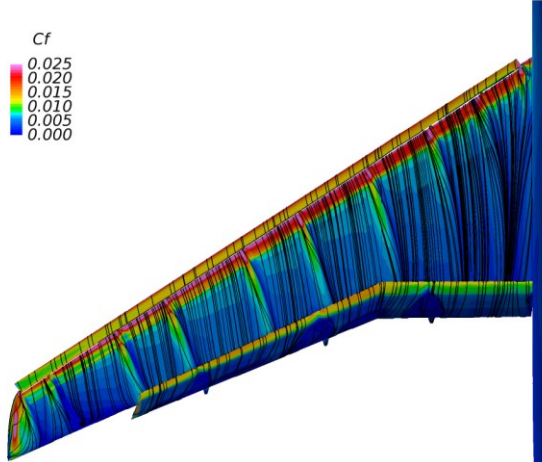
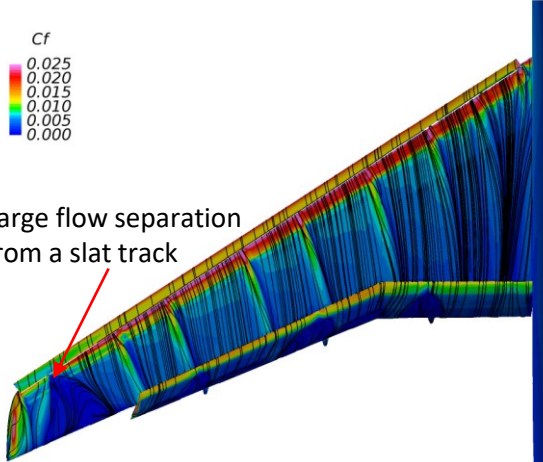
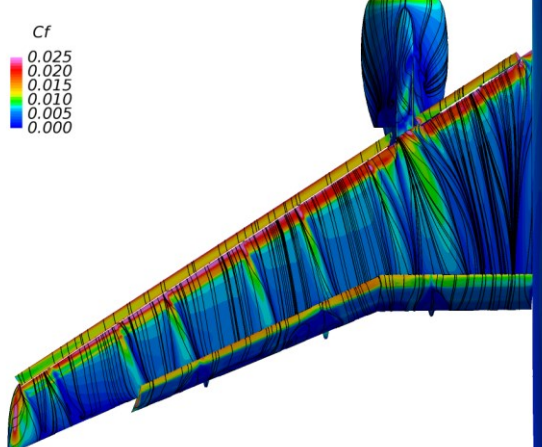
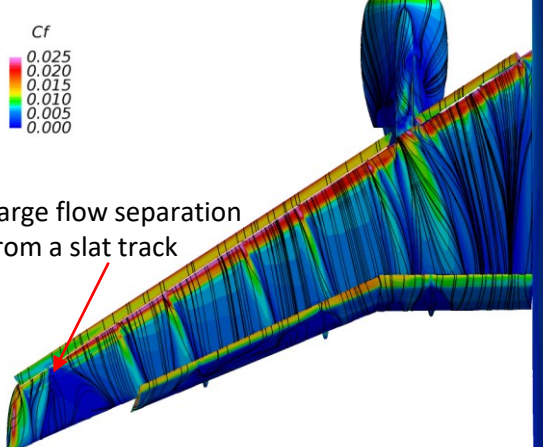
- QCR on/off predict similar C_p distributions except at the outboard section.
- QCR off agrees better with experiment even at H-H section.

— QCR off
— QCR on



Cases 2a & 2c – JSM $\alpha = 14.54^\circ$

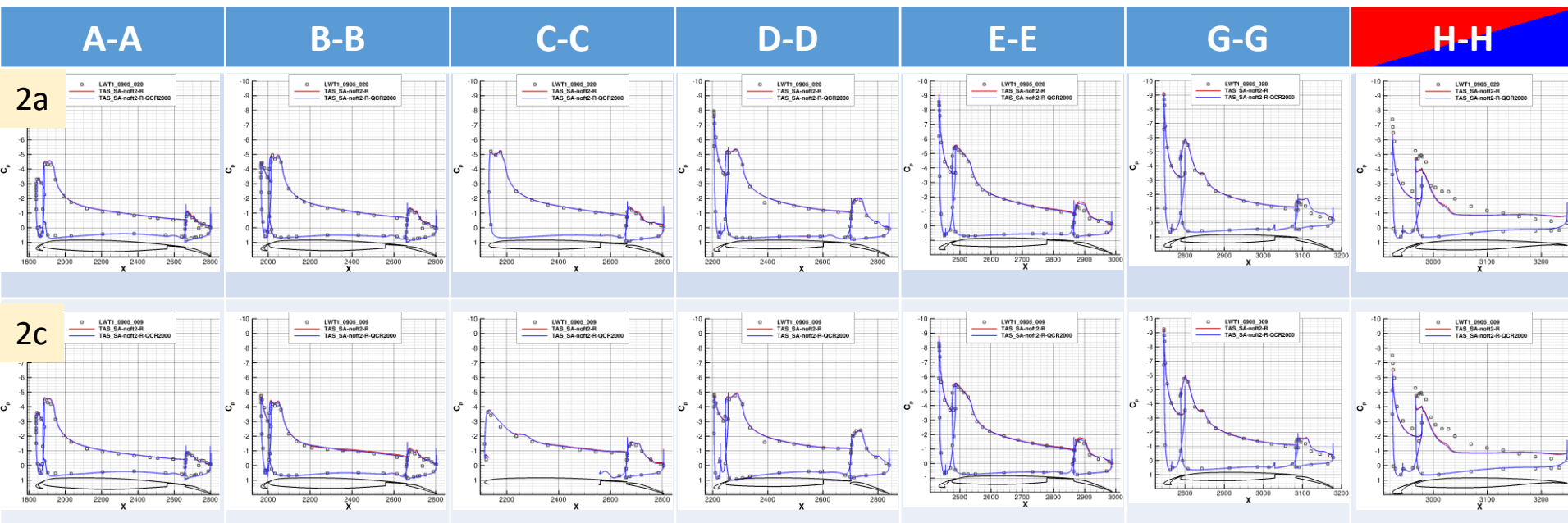
- Difference in the size of flow separation between QCR on & off

Exp	QCR off	QCR on
<p>Case 2a</p> <p><i>No oil flow images available</i></p>		 <p>Large flow separation from a slat track</p>
<p>Case 2c</p> <p><i>No oil flow images available</i></p>		 <p>Large flow separation from a slat track</p>

Cases 2a & 2c – JSM $C_p \alpha = 18.58^\circ$

- QCR on/off predict similar C_p distributions and large flow separation at H-H section, which was not observed in the experiment.

— QCR off
— QCR on



Cases 2a & 2c – JSM $\alpha = 18.58^\circ$

- Difference in the size of flow separation between CFD & WTT

Exp

QCR off

QCR on

Case 2a

C_f
0.025
0.020
0.015
0.010
0.005
0.000

Larger flow separation
from a slat track

C_f
0.025
0.020
0.015
0.010
0.005
0.000

Larger flow separation
from a slat track

Case 2c

C_f
0.025
0.020
0.015
0.010
0.005
0.000

Larger flow separation
from a slat track

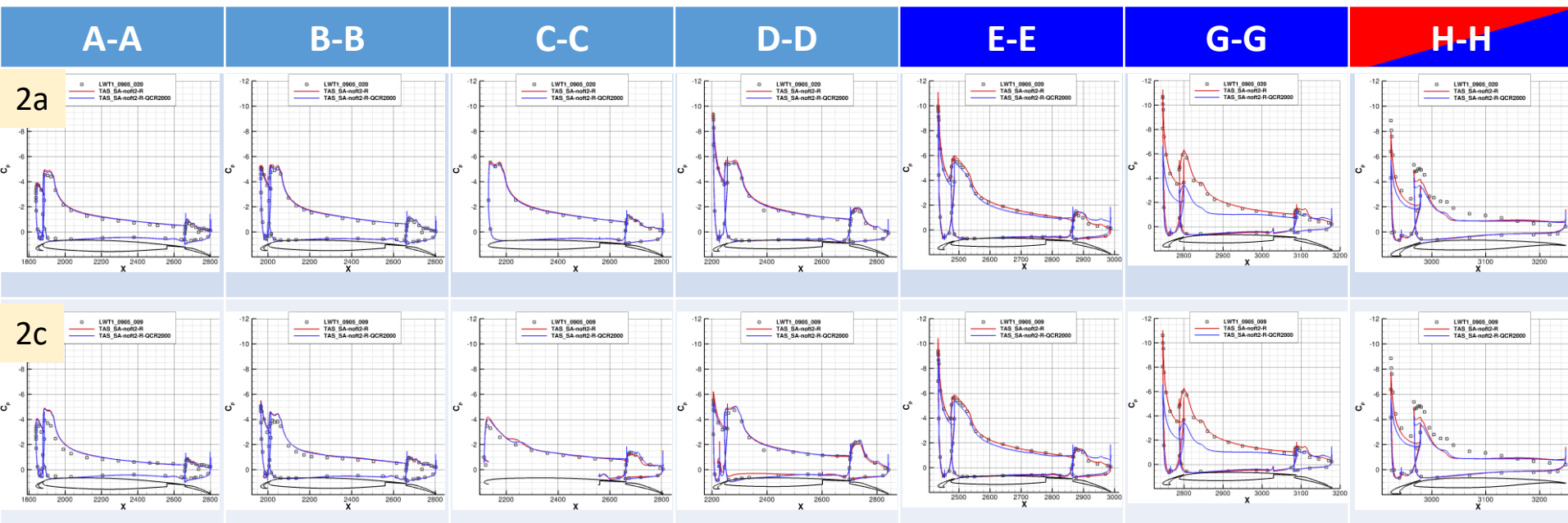
C_f
0.025
0.020
0.015
0.010
0.005
0.000

Larger flow separation
from a slat track

Cases 2a & 2c – JSM $C_p \alpha = 20.59^\circ$

- QCR on predicts large flow separation on the outboard wing.
- QCR off also predicts large flow separation at H-H section.

— QCR off
— QCR on



Cases 2a & 2c – JSM $\alpha = 20.59^\circ$



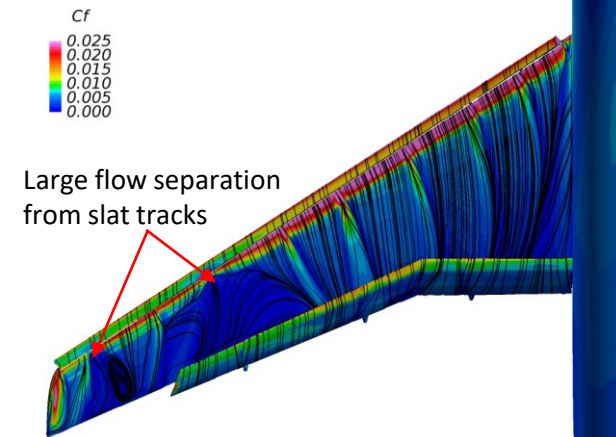
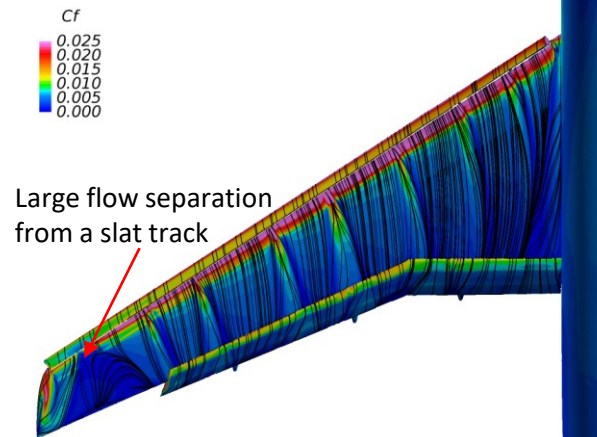
Exp

QCR off

QCR on

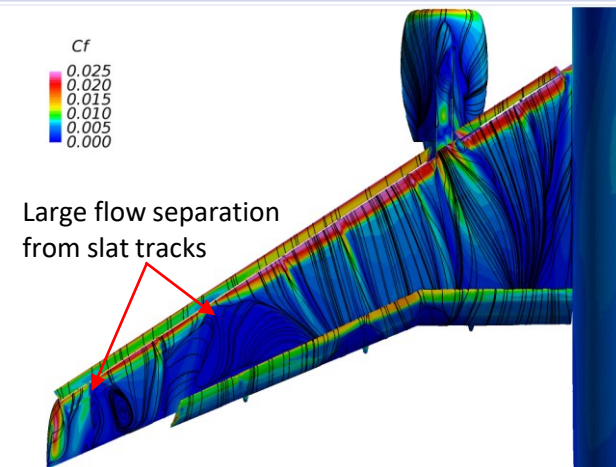
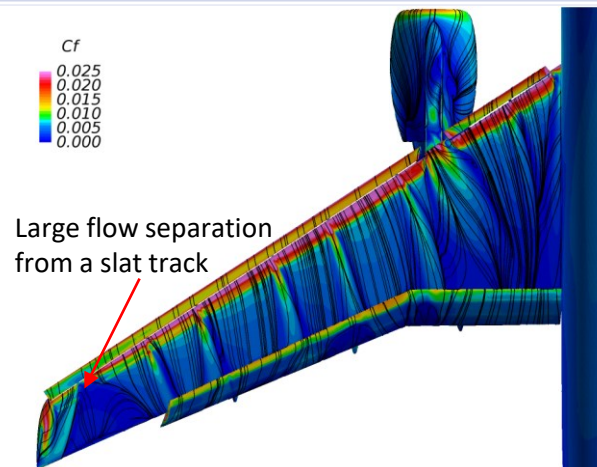
Case 2a

*No oil flow
images available*



Case 2c

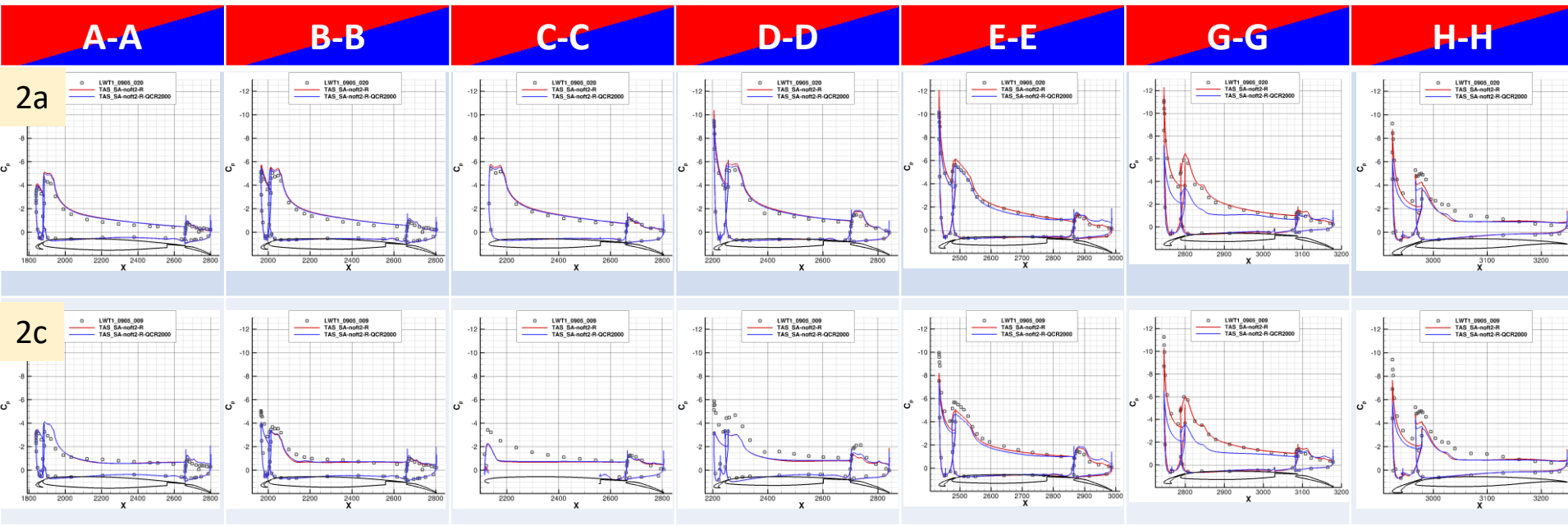
*No oil flow
images available*



Cases 2a & 2c – JSM $C_p \alpha = 21.57^\circ$

- QCR on/off predict slightly different C_p distributions even at inboard sections.
- QCR off predicts better C_p distribution at G-G section.

— QCR off
— QCR on



Cases 2a & 2c – JSM $\alpha = 21.57^\circ$

- Difference in the size of flow separation between CFD & WTT

Exp

Case 2a

Large SOB flow separation

QCR off

C_f
0.025
0.020
0.015
0.010
0.005
0.000

QCR on

C_f
0.025
0.020
0.015
0.010
0.005
0.000

Large flow separation from a slat track

Case 2c

Large SOB flow separation

C_f
0.025
0.020
0.015
0.010
0.005
0.000

Large flow separation from the pylon

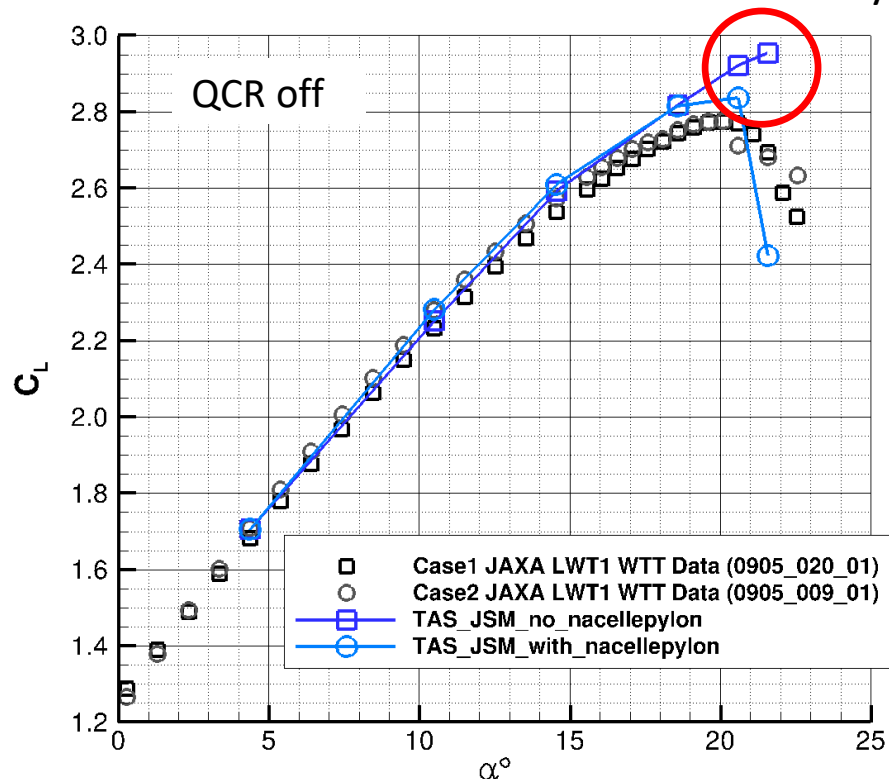
C_f
0.025
0.020
0.015
0.010
0.005
0.000

Large flow separation from the pylon

Large flow separation from a slat track

Case 2a JSM C_L - α

- QCR off agreed better with experiment in Cases 2a & 2c.
- QCR off predicted higher $C_{L_{max}}$ with the JAXA medium grid.
 - Does the laminar-to-turbulent transition need to be considered?
 - JAXA has provided the info.
 - Does wing deformation influence the prediction?
 - How about the mesh density?



Case 2a JSM Wing Deformation for Meshes

- Polynomial approximation using displacement data measured at 32 markers on the main wing element in a wind tunnel test.

- Quartic approximation to estimate wing bending and twisting

- Yasue, K. and Ueno, M., "Model Deformation Corrections of NASA Common Research Model Using Computational Fluid Dynamics," *Journal of Aircraft*, Vol. 53, No. 4, July 2016, pp. 951-961, DOI: 10.2514/1.c033445.
- Le Sant, Y. "A Model Deformation Method Applied to PSP Measurements," Proceedings of the 20th International Congress on Instrumentation in Aerospace Simulation Facilities, 2003.

$$x_d = x_a, y_d = y_a,$$

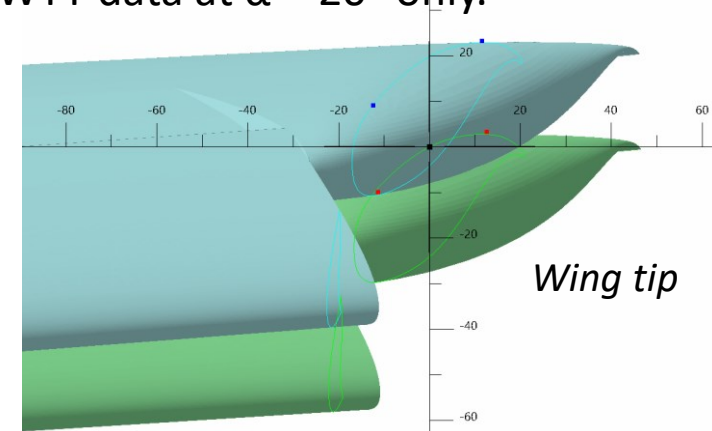
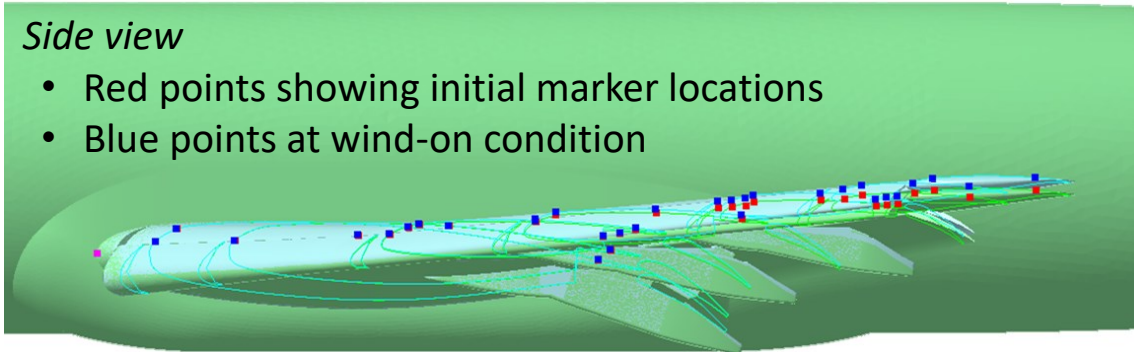
$$z_d = z_a + y_a^2 o_2 + y_a^3 o_3 + y_a^4 o_4 + x_a y_a t_1 + x_a y_a^2 t_2 + x_a y_a^3 t_3 + x_a y_a^4 t_4$$

$\mathbf{x}_a = (x_a, y_a, z_a)$ and \mathbf{x}_d are in the coordinate system obtained by rotating the initial coordinate system around the x-axis by the wing dihedral angle, 3.0°.

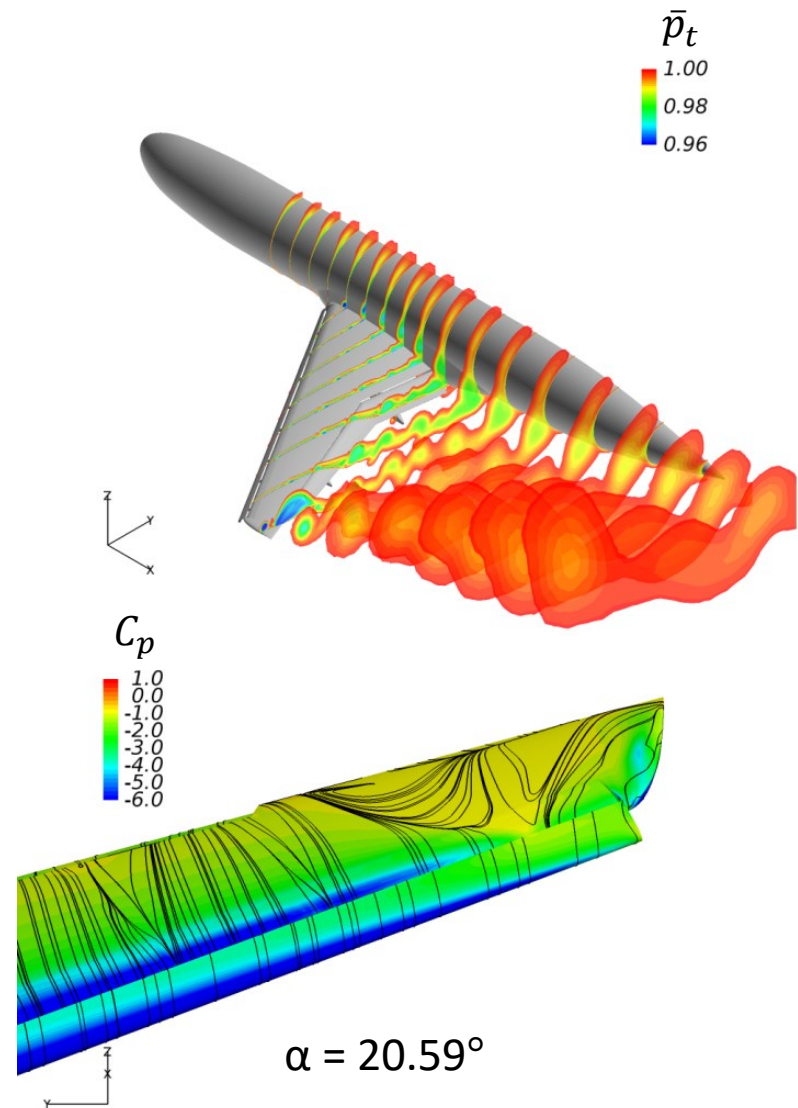
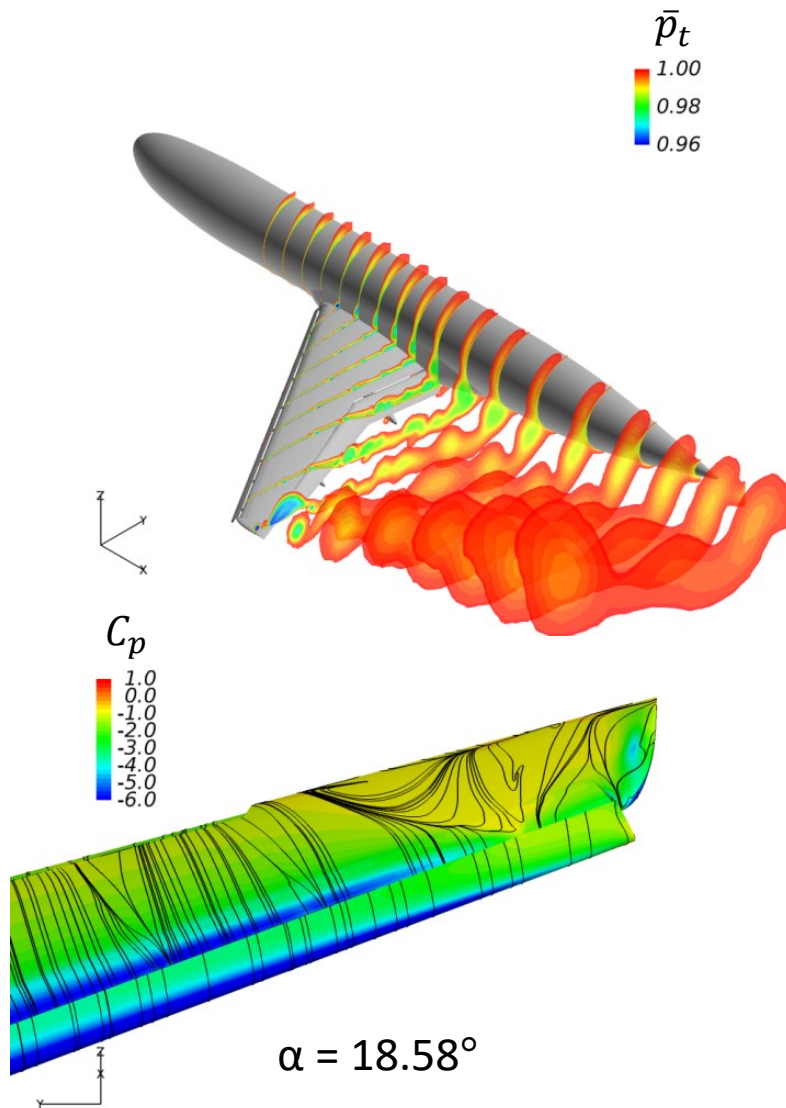
- Only $y < -311.9$ mm is deformed.
- Gap, overlap and deflection angle of the slat and the flap are not changed.
- Currently, Case 2a (nacelle/pylon off) using WTT data at $\alpha = 20^\circ$ only.

Side view

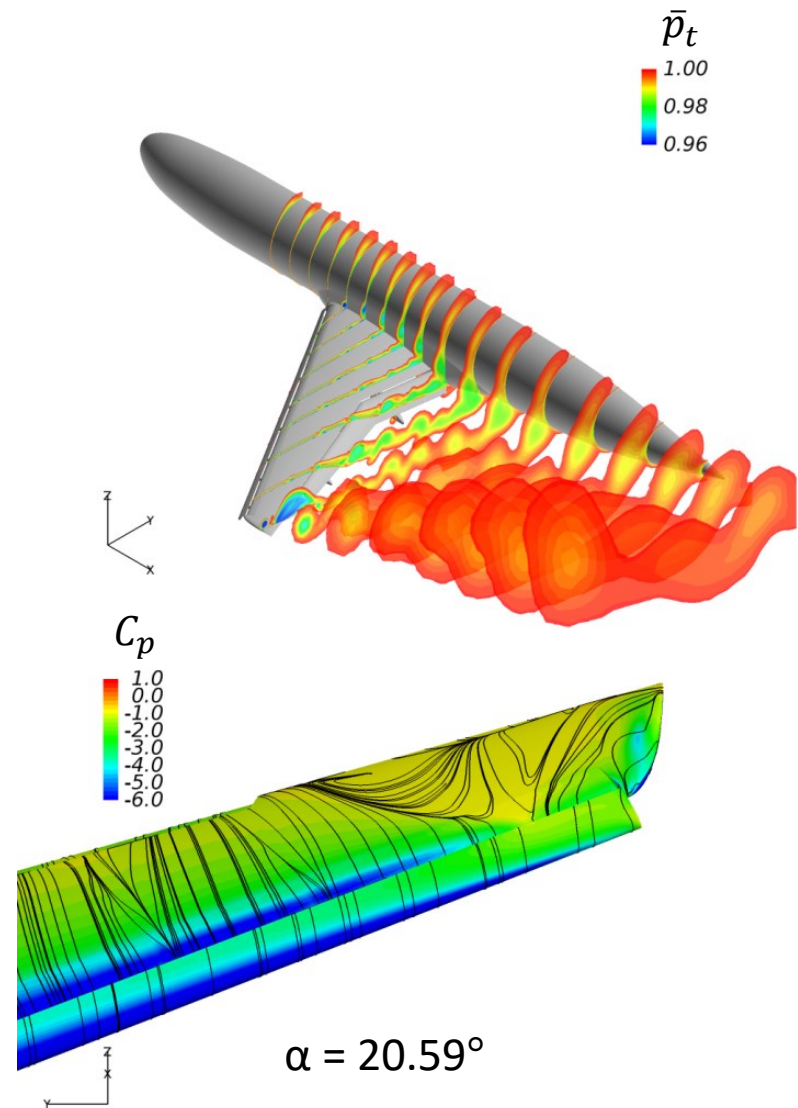
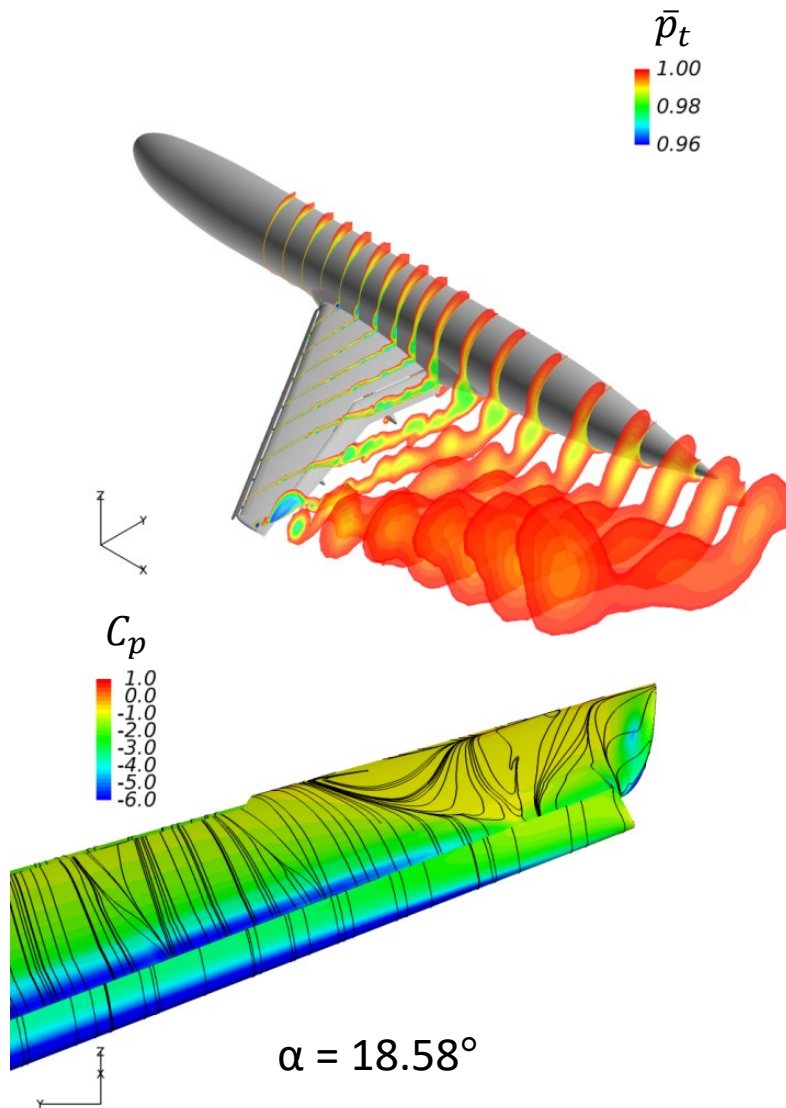
- Red points showing initial marker locations
- Blue points at wind-on condition



Case 2a JSM – No Wing Deformation

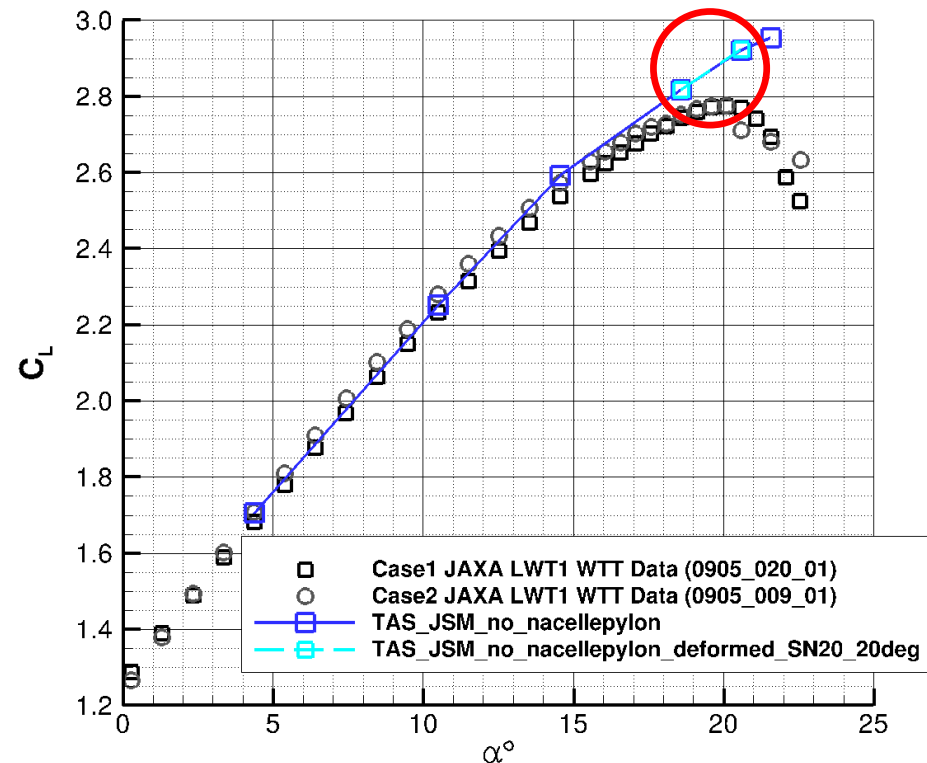
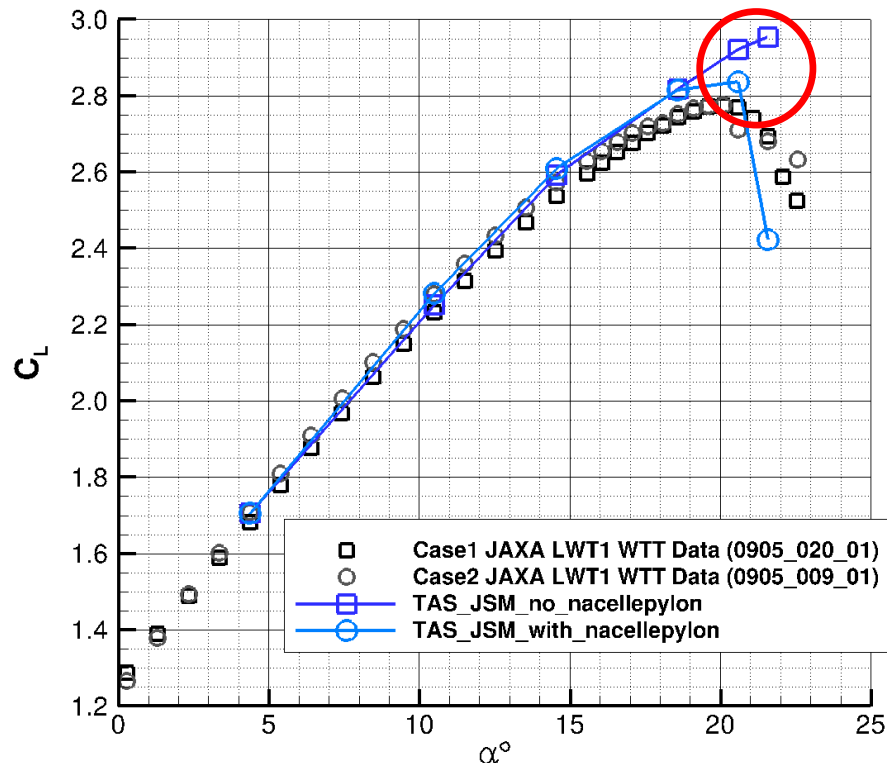


Case 2a JSM – Wing Deformation Applied



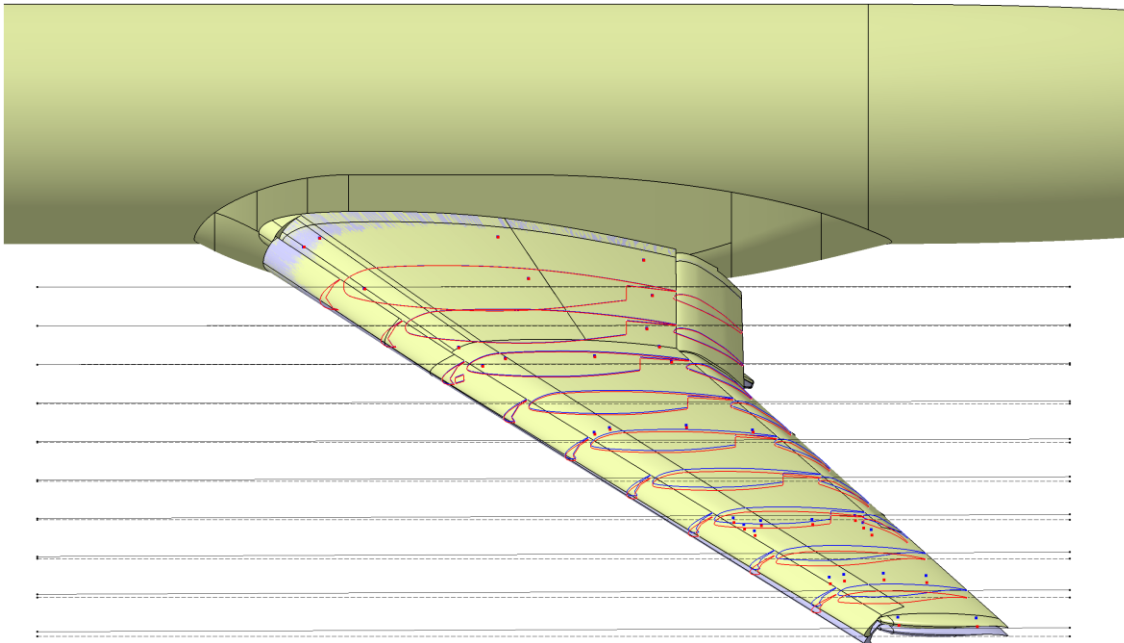
Case 2a JSM – C_L - α

- TAS code predicted higher $C_{L_{max}}$ with JAXA medium grid.
- Does wing deformation influence the prediction?
 - No, according to TAS code with the medium grid for Case 2a.
 - Finer meshes are needed for further evaluation.



Cases 2a & 2c JSM Wing Deformation for CAD Model

- The same polynomial approximation is applied to CAD models on CATIA by defining 10 sections on the wing reference plane (WRP).
 - Case 2a (nacelle/pylon off) at $\alpha = 4^\circ, 10^\circ, 14^\circ, 20^\circ, 21^\circ$
 - Case 2c (nacelle/pylon on) at $\alpha = 4^\circ, 10^\circ, 14^\circ, 18^\circ, 20^\circ, 21^\circ$
- The deformed CAD models to be released for public.

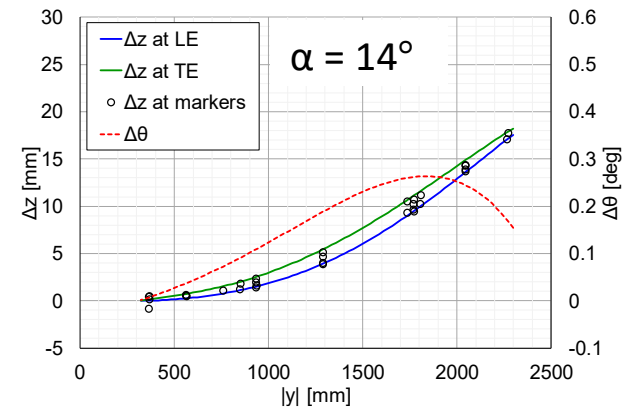
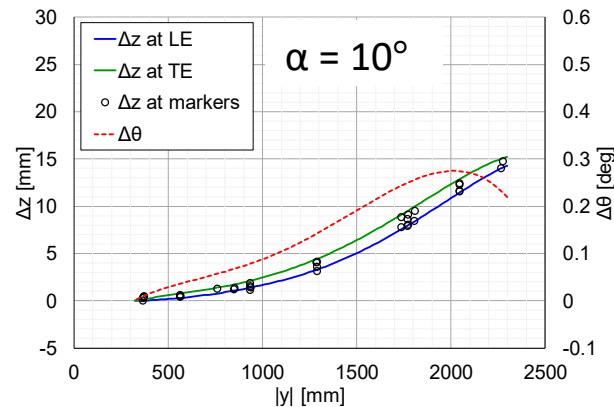
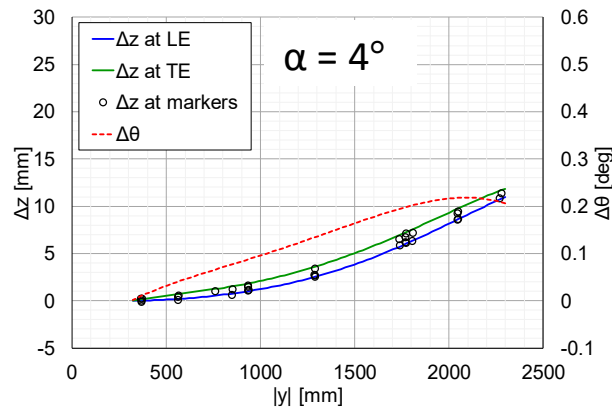


- Example: Case 2a at $\alpha = 21^\circ$
- Before deformation:
 - Black dashed lines on WRP & corresponding red sections
 - Red dots from a wind tunnel test as reference
- After deformation:
 - Black solid lines on WRP & corresponding blue sections
 - Blue dots from a wind tunnel test

Case 2a (nacelle/pylon off) JSM Deformed CAD Models

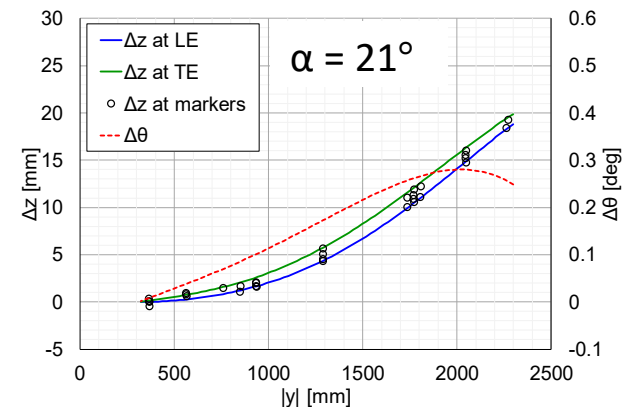
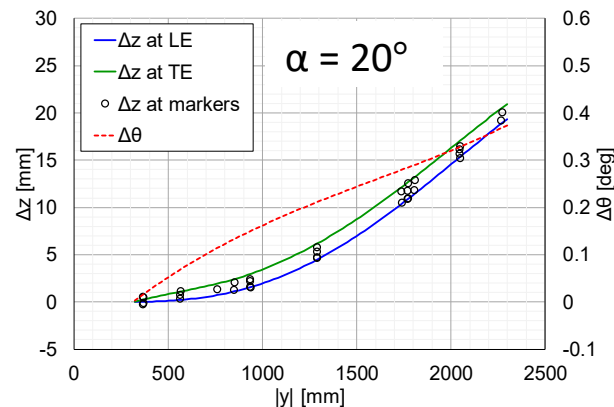


- Displacement in the z direction Δz at the retracted wing leading and trailing edges and change in twist angle $\Delta\theta$



$\alpha = 18^\circ$

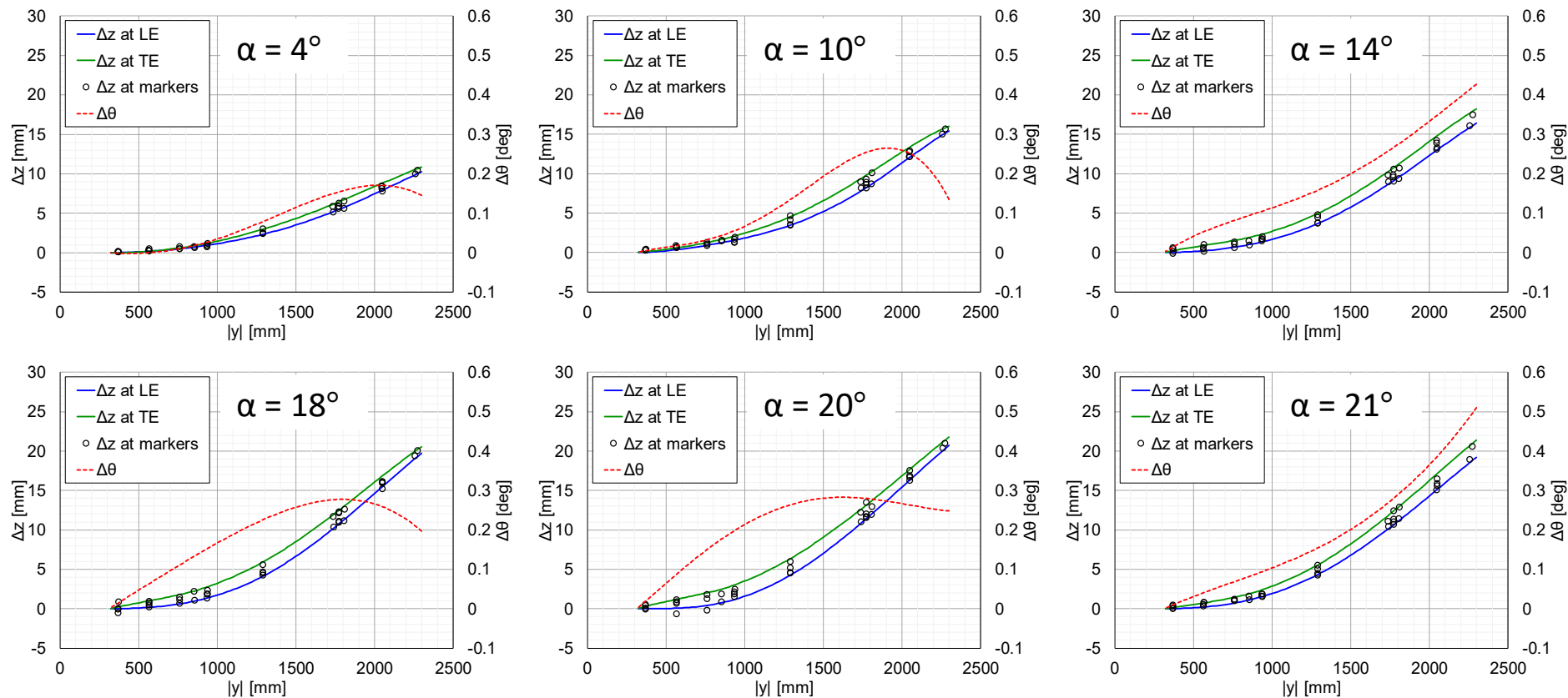
Not available



Case 2c (nacelle/pylon on) JSM Deformed CAD Models



- Displacement in the z direction Δz at the retracted wing leading and trailing edges and change in twist angle $\Delta\theta$



Summary

- Large flow separation was observed on the HL-CRM flaps, but with the B3 fine mesh, much smaller separation was observed at $\alpha = 16^\circ$.
- When QCR in the SA turbulence model is turned on,
 - Slightly larger flow separation was observed with HL-CRM and JSM, which was similar to the HiLiftPW-2 DLR F11 cases.
 - Large flow separation was observed from JSM slat tracks at high α .
- JSM wing without nacelle/pylon was deformed based on marker displacement measurements in a wind tunnel test at $\alpha = 20^\circ$.
 - No significant effect was observed in aerodynamic coefficients with the JAXA medium grid.
 - Cases 2a & 2c JSM CAD models were deformed at several angles of attack for public release, to be available on the HiLiftPW web site shortly.
 - The effect of mesh density needs to be evaluated.